Slow optical soliton pairs via electron spin coherence in a quantum well waveguide

Ji-Bing Liu,* Na Liu, Chuan-Jia Shan, Tang-Kun Liu, and Yan-Xia Huang
Department of Physics, Hubei Normal University, Huangshi 435002, China

(Received 2 November 2009; revised manuscript received 27 December 2009; published 24 March 2010)

In this paper, we theoretically investigate the propagation properties of probe and mixing fields in a quantum well waveguide. This waveguide is driven by two strong control (pumping and coupling) fields and a weak probe field. Under appropriate parameters condition, the electron spin coherence can suppress the absorption and enhance the nonlinear susceptibilities of the probe (or mixing) field. This study reveals that probe (or mixing) field can form soliton pairs and propagate in the quantum well waveguide with slow group velocity. We also study the soliton collision and dynamics evolution. The results show that the propagation of soliton can be strongly modified by the electron spin coherence.

DOI: 10.1103/PhysRevE.81.036607 PACS number(s): 42.65.Tg, 42.50.Gy, 78.67.De

I. INTRODUCTION

In recent years, people have paid considerable attentions to the study of electron spin coherence in semiconductors. This may be due to its long spin-coherence times which have been observed in *n*-doped semiconductors [1,2]. Previous work demonstrated that the ability to control electron spin states in semiconductors is important in spintronics and quantum information processing [3–6], so it is necessary to fast and coherently manipulate local spin states and to control and operate spin coherence in semiconductor nanostructures [7–10]. Wu *et al.* [11] used picosecond pulses to display phase-sensitive partial rotations of the electron spin vector in an ensemble of singly charged quantum dots. Mikkelsen *et al.* [12] used time-resolved Kerr rotation spectroscopy to monitor the coherent evolution of an electron spin in a single-quantum dot. Chen *et al.* [13] investigated the effects of disorder on electron spin dynamics in a semiconductor quantum well and determined the density of states by measuring the electron Landé *g*-factor dependence on density. Their results showed that the weakly localized spin has the longer spin coherence.

On the other hand, there has been substantial research interest in the investigation of quantum coherence in atomic and semiconductor media. Many interesting physical phenomena have been demonstrated such as electromagnetically induced transparency (EIT) [14–20], lasing without inversion [21–23], slow and stopped light [24], and stimulated Raman adiabatic passage [25]. Quantum coherence cannot only modify the linear absorption and dispersion properties, but also enhance the nonlinear optical processes such as highly efficient four-wave mixing [26–28] and ultraslow optical soliton [29].

Optical soliton represents a fascinating manifestation of nonlinear phenomena in nature and receives a great deal of attention. Because the formation of temporal and spatial soliton can preserve shape propagation in nonlinear media, soliton can occur in many states of matter such as optical fiber [30,31], semiconductor [32,33], molecular magnets [34,35], Bose-Einstein condensed atomic vapor [36–39], and cold atomic medium [29,40,41]. Especially, theoretical study shows that the life-broadened atom media can support the propagation of a new class of two-color ultraslow and superluminal optical solitons [42,43]. And the research of the temporal [44–46] and spatial [47–49] vector optical solitons also has received much attention because of the promising applications for the design of new types of all-optical switches and logic gates. Recently, ultraslow temporal vector optical solitons in a cold atomic medium under Raman excitation have been discussed and the ultraslow Manakov temporal vector optical solitons can be realized by adjusting the Rabi frequencies of the control fields [50].

There have been several studies about the EIT and slow light propagation in systems of semiconductor quantum well (QW) waveguide (WG) via electron spin coherence. Li *et al.* [51] proposed a theoretical scheme to realize EIT via robust electron spin coherence in a semiconductor quantum well waveguide. Their results displayed that the EIT in the waveguide is strongly modified by the electron spin coherence. Chang *et al.* [52] investigated the slow light phenomenon in a quantum well waveguide using EIT. They pointed out that the electron spin coherence and the strain-induced can enhance the performance of slow light. Palinginis *et al.* [53] experimentally realized slow light propagation via coherent population oscillation in a GaAs quantum well waveguide. Yang *et al.* [54] proposed a theoretical scheme to realize four-wave mixing via electron spin coherence in a waveguide. Their results displayed that electromagnetically induced absorption and superluminal propagation could be realized in the waveguide at room temperatures.

In this paper, we discuss the propagation properties of the weak probe (or mixing) field and the formation of slow soliton pairs in a quantum well waveguide which the electron spin coherence is considered. In general, the photon does not strongly couple to the spin degree of freedom, but it is possible to use spin-orbit coupling in the quantum well waveguide to generate spin polarized distributions. So interband dipole optical transitions between the doubly degenerate heavy-hole (hl) ($J_z=\pm 3/2$) and light-hole (lh) ($J_z=\pm 1/2$) valence bands and the doubly generate conduction bands ($S_z=\pm 1/2$), respectively. Figure 1 shows the schematic of energy levels and the corresponding dipole-allowed transitions. The electron spin coherence is induced through the transition from $|a\rangle$ to $|b\rangle$ and $|b\rangle$ to $|d\rangle$. Such a model with

*Corresponding author; jibl@foxmail.com

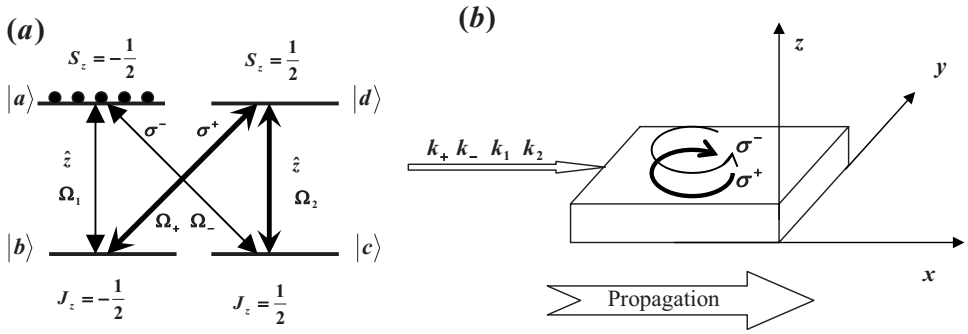

FIG. 1. (a) The schematic of energy levels. The valence-band states are labeled with J_z and the conduction-band states are labeled with $S_z=\frac{1}{2}$ (spin up) and $S_z=-\frac{1}{2}$ (spin down). This sample interacts with the σ^+ polarized field (Ω_+) and the linear polarized field (Ω_2) serving as the strong pump lasers, and the σ^- polarized probe field (Ω_-) and the generating mixing field (Ω_1) serving as the weak fields. Here, $2\Omega_j$ ($j=1,2,\pm$) denote the corresponding Rabi frequency, respectively. (b) Definition of coordinate frame and polarization configuration for the pump-probe fields. The linear polarized field is polarized along the z axis (the growth direction) and light propagates in the x direction.

the electron spin coherence has many interesting nonlinear optical processes such as EIT [51], slow light [52,53], and four-wave mixing [54]. However, the previous theoretical and experimental works studying do not include the formation of slow optical soliton pairs. We focus on the evolution of weak field, absorption, dispersion, and the optical Kerr nonlinearity effect. Finally, we will show that slow soliton pairs can form and propagate in the waveguide. To the best our knowledge, such slow optical soliton pairs in a quantum well waveguide with the electron spin coherence have never been studied.

It is noted that electron spin coherence can arise through a coherent superposition of two spin states in the conduction band of a semiconductor quantum well. More recent studies have displayed that conduction-electron spin coherence has a very long decoherence time compared to other forms of quantum coherence [5]. In semiconductors, electron spin coherence can be preserved over remarkably long time and length scales. Especially, electron spin coherence can persist to room temperature [2,55]. This fact and our present results indicate that slow soliton pairs may be realized in semiconductor quantum well at room temperatures. Due to these robust qualities, electron spin coherence promises to be an excellent model system for exploring coherent quantum phenomena in semiconductors.

Some literatures have been proposed to investigate ultraslow optical soliton pairs in atomic systems [42,43]. Even in semiconductor quantum well system, this is motivated by studying the nonlinear phenomena through the gas of four-level cold atoms [42,43,56]. However, there are some differences between the two situations. Firstly, the medium studied here is solid, which is much more practical than that in atomic media. Secondly, semiconductor quantum well system has high nonlinear optical coefficients and large electric-dipole moments of lh transitions due to the small effective electron mass. In semiconductor, electron spin coherence has a smaller decoherence rate than the other forms of quantum coherence, so the robustness of the electron spin coherence can make it as a highly promising platform for optical manipulation of quantum coherence and the development of coherent quantum devices.

II. MODEL AND EQUATION OF MOTION

Let us consider a double V-type quantum well waveguide system as shown in Fig. 1. To include electron spin coherence, a strong field, which is polarized along the z axis, drives the transition from $|c\rangle$ to $|d\rangle$ and a weak probe field, which is σ^- polarized, drives the transition from $|c\rangle$ to $|a\rangle$. The electron spin coherence can also be induced through the transition from $|b\rangle$ to $|a\rangle$, which is driven by the mixing field, and the transition from $|b\rangle$ to $|d\rangle$, which is driven by the second strong σ^+ polarized field. Consequently, we have a coupled double-V scheme. The semiconductor quantum well WG structure, considered here, consists of a (110) GaAs substrate, 1.18 μm of $Al_{0.29}Ga_{0.71}As$ (WG cladding), 0.17 μm of $Al_{0.15}Ga_{0.85}As$ (WG core), 0.40 μm $Al_{0.30}Ga_{0.70}As$ (WG cladding), 60 nm $Al_{0.3}Ga_{0.7}As$ (barrier), 13 nm GaAs (QW), and a 20 nm GaAs cap layer. The overall structure provides a planar waveguide [57]. We presume that the lateral extension of the waveguide is much greater than the optical wavelength and the fundamental mode can approximately be recognized as a plane wave. As explained in Ref. [51], the electron spin coherence can greatly change the absorption and dispersion of probe field in the semiconductor quantum well structure. The effects of the two light-hole coherence can be neglected because the nonradiative coherence between the two light-hole valence bands decays quickly than electron spin coherence. This system has been experimentally realized in a semiconductor quantum well waveguide [53]. Taking the dipole and rotating wave approximation, in the interaction picture, the Hamiltonian can be written as

$$\begin{aligned}\hat{H}_{int}^{I}/\hbar = {} & \Delta_1|b\rangle\langle b| + \Delta_-|c\rangle\langle c| + (\Delta_- - \Delta_2)|d\rangle\langle d| \\ & - (\Omega_- e^{i\vec{k}_-\cdot\vec{r}}|a\rangle\langle c| + \Omega_+ e^{i\vec{k}_+\cdot\vec{r}}|d\rangle\langle b| + \text{H.c.}) \\ & - (\Omega_1 e^{i\vec{k}_1\cdot\vec{r}}|a\rangle\langle b| + \Omega_2 e^{i\vec{k}_2\cdot\vec{r}}|d\rangle\langle c| + \text{H.c.}), \end{aligned} \quad (1)$$

where the detunings are defined as $\Delta_1=\omega_1-\omega_{ab}$, $\Delta_-=\omega_--\omega_{ac}$, and $\Delta_2=\omega_2-\omega_{dc}$. Here, $\omega_{mn}=(\epsilon_m-\epsilon_n)/\hbar$ $[m,n=a,b,c,d;\ m\neq n;\ \epsilon_{m(n)}$ is the energy of state $|m(n)\rangle]$, ω_j $(j=1,2,\pm)$ is the frequency of the corresponding laser, and $\Omega_+=(\vec{\mu}_{bd}\cdot\vec{e}_+)E_+/\hbar$, $\Omega_-=(\vec{\mu}_{ac}\cdot\vec{e}_-)E_-/\hbar$,

$\Omega_1=(\vec{\mu}_{ab}\cdot\vec{e}_1)E_1/\hbar$ and $\Omega_2=(\vec{\mu}_{dc}\cdot\vec{e}_2)E_2/\hbar$ are the corresponding Rabi frequencies with $\vec{\mu}_{mn}$ being the dipole moment for the relevant transition $|m\rangle\leftrightarrow|n\rangle$, $E_j(j=\pm,1,2)$ being the corresponding electric field amplitude, and $\vec{e}_j$ being the polarization unite vector of the electric field. By adopting the standard approach [58] and including the coherent wave mixing process, we can write the density-matrix elements as follows:

$$\dot{\rho}_{bb}=-\gamma_{2l}\rho_{bb}+i\Omega_1^*\rho_{ab}-i\Omega_1\rho_{ba}+i\Omega_+^*\rho_{db}-i\Omega_+\rho_{bd}, \tag{2a}$$

$$\dot{\rho}_{cc}=-\gamma_{1l}\rho_{cc}+i\Omega_-^*\rho_{ac}-i\Omega_-\rho_{ca}+i\Omega_2^*\rho_{dc}-i\Omega_2\rho_{cd}, \tag{2b}$$

$$\dot{\rho}_{dd}=-\gamma_{3l}\rho_{dd}+i\Omega_+\rho_{bd}-i\Omega_+^*\rho_{ba}+i\Omega_2\rho_{cd}-i\Omega_2^*\rho_{dc}, \tag{2c}$$

$$\dot{\rho}_{ac}=i(\Delta_-+i\gamma_1)\rho_{ac}+i\Omega_-(\rho_{cc}+\rho_{aa})-i\Omega_2\rho_{ad}+i\Omega_1\rho_{bc}, \tag{2d}$$

$$\dot{\rho}_{ab}=i(\Delta_1+i\gamma_2)\rho_{ab}+i\Omega_1(\rho_{bb}-\rho_{aa})+i\Omega_-\rho_{cb}-i\Omega_+\rho_{ad}, \tag{2e}$$

$$\dot{\rho}_{ad}=i[(\Delta_--\Delta_2)+i\gamma_3]\rho_{ad}+i\Omega_1\rho_{bd}+i\Omega_-\rho_{cd}-i\Omega_+^*\rho_{ab}-i\Omega_-\rho_{ac}, \tag{2f}$$

$$\dot{\rho}_{bd}=i[(\Delta_--\Delta_2-\Delta_1)+i\gamma_4]\rho_{bd}+i\Omega_+^*(\rho_{dd}-\rho_{bb})-i\Omega_2^*\rho_{bc}+i\Omega_1^*\rho_{ad}, \tag{2g}$$

$$\dot{\rho}_{bc}=i[(\Delta_--\Delta_1)+i\gamma_5]\rho_{bc}-i\Omega_-\rho_{ba}-i\Omega_2\rho_{bd}+i\Omega_+^*\rho_{dc}+i\Omega_1^*\rho_{ac}, \tag{2h}$$

$$\dot{\rho}_{cd}=i(\Delta_2+i\gamma_6)\rho_{cd}+i\Omega_-^*\rho_{ad}+i\Omega_2^*\rho_{dd}-i\Omega_+^*\rho_{cb}-i\Omega_2^*\rho_{cc}, \tag{2i}$$

$$\rho_{aa}+\rho_{bb}+\rho_{cc}+\rho_{dd}=1, \tag{2j}$$

where γ_i $(i=1-6)$ denote the total dephasing rates, which are phenomenologically added. We have utilized the phase matching condition $\vec{k}_1=\vec{k}_+-\vec{k}_--\vec{k}_2$. The overall dephasing rates $\gamma_i(i=1,2)$ are defined by $\gamma_1=(\gamma_{cl}+\gamma_{ca}^d)/2$, $\gamma_2=(\gamma_{bl}+\gamma_{ba}^d)/2$, $\gamma_3=(\gamma_{dl}+\gamma_{da}^d+\gamma_d)/2\simeq\gamma_d/2$, $\gamma_4=(\gamma_{bl}+\gamma_{dl}+\gamma_{bd}^d)/2$, $\gamma_5=(\gamma_{bl}+\gamma_{cl}+\gamma_{bc}^d)/2$, and $\gamma_6=(\gamma_{dl}+\gamma_{cl}+\gamma_{cd}^d)/2$. γ_{jl} is due to longitudinal optical photon emission events at low temperature, γ_{ij}^d may originate not only from electron-electron scattering and electron-phonon scattering, but also from inhomogeneous broadening due to the scattering on interface roughness, and γ_d is the decay rate for the spin coherence. Then, under the slowly varying envelope approximation, the evolution equation for the slowly varying amplitudes

$$\frac{\partial}{\partial x}\Omega_1+\frac{1}{c}\frac{\partial}{\partial t}\Omega_1=i\frac{N\omega_1|\mu_{ab}|^2\rho_{ab}}{2\hbar c\epsilon_0}, \tag{3a}$$

$$\frac{\partial}{\partial x}\Omega_-+\frac{1}{c}\frac{\partial}{\partial t}\Omega_-=i\frac{N\omega_-|\mu_{ac}|^2\rho_{ac}}{2\hbar c\epsilon_0}, \tag{3b}$$

where N is an effective density averaged over the cross section of the probe field. Supposing the probe and mixing fields are weak, the control (coupling and pumping) fields are strong enough, and the system is initially in the electron state $|a\rangle$, so we can adopt a perturbation treatment for obtaining the approximation solution. The pumping field and coupling field are strong enough to make $\epsilon=\Omega_{1(-)}/\Omega_{2(+)}$ be a small parameter. Within an adiabatic framework, we make the asymptotic expansion $\rho_{mn}=\Sigma_k\rho_{mn}^{(k)}$ ($\rho_{mn}^{(k)}$ is the kth-order part of $\rho_{mn},m,n=a,b,c,d$) and $\rho_{ma}^{(k)}\sim\epsilon^k$. Then, the approximation solutions, up to the first order in the weak fields ($\Omega_{1(-)}$), are given as

$$\rho_{ab}^{(1)}\simeq\frac{(R_1'R_3'-|\Omega_2|^2)\Omega_1+\Omega_+\Omega_2^*\Omega_-}{R_1'R_2'R_3'-R_1'|\Omega_+|^2-R_2'|\Omega_2|^2}, \tag{4a}$$

$$\rho_{ac}^{(1)}\simeq\frac{\Omega_2\Omega_+^*\Omega_1+(R_2'R_3'-|\Omega_+|^2)\Omega_-}{R_1'R_2'R_3'-R_1'|\Omega_+|^2-R_2'|\Omega_2|^2}, \tag{4b}$$

$$\rho_{ad}^{(1)}\simeq\frac{R_1'\Omega_+^*\Omega_1+R_2'\Omega_2^*\Omega_-}{R_1'R_2'R_3'-R_1'|\Omega_+|^2-R_2'|\Omega_2|^2}, \tag{4c}$$

where $R_1'=\Delta_-+i\gamma_1$, $R_2'=\Delta_1+i\gamma_2$, and $R_3'=(\Delta_--\Delta_2)+i\gamma_3$. Before considering the nonlinear evolution of weak probe and mixing fields, we first analyze the relevant linearized results by neglecting the nonlinear term in the right-hand side of Eqs. (3a) and (3b). Performing Fourier transform for Eqs. (3a) and (3b), we obtain the solutions for probe and mixing fields

$$\Lambda_-(x,\omega)=\frac{\Lambda_-(0,\omega)\{U_+\exp[ixK_+(\omega)]-U_-\exp[ixK_-(\omega)]\}}{U_+(\omega)-U_-(\omega)}, \tag{5a}$$

$$\Lambda_1(x,\omega)=\frac{\Lambda_-(0,\omega)\{\exp[ixK_+(\omega)]-\exp[ixK_-(\omega)]\}}{U_+(\omega)-U_-(\omega)}, \tag{5b}$$

where $\Lambda_-(x,\omega)$ and $\Lambda_1(x,\omega)$ are the Fourier transforms of Ω_- and Ω_1, respectively. We have used the initial condition for generating mixing field, $\Lambda_1(0,\omega)=0$, when we obtain Eqs. (5a) and (5b). $\Lambda_-(0,\omega)$ is the Fourier transform of $\Omega_-(0,t)$ and $\Omega_-(0,t)$ is the probe field at the entrance $x=0$. The expressions of $U_\pm(\omega)$ and $K_\pm(\omega)$ read

$$K_\pm(\omega)=\frac{\omega}{c}+\frac{\kappa_{ab}(R_1R_3-|\Omega_2|^2)+\kappa_{ac}(R_2R_3-|\Omega_+|^2)\pm\sqrt{S(\omega)}}{R_1R_2R_3-R_1|\Omega_+|^2-R_2|\Omega_2|^2}=K_\pm^{(0)}+K_\pm^{(2)}\omega+K_\pm^{(2)}\omega^2+\cdots, \tag{6a}$$

$$U_\pm(\omega)=\frac{\kappa_{ac}(R_2R_3-|\Omega_+|^2)-\kappa_{ab}(R_1R_3-|\Omega_2|^2)\pm\sqrt{S(\omega)}}{2\kappa_{ab}\Omega_+\Omega_2^*}=U_\pm^{(0)}+U_\pm^{(1)}\omega+O(\omega^2), \tag{6b}$$

where $\kappa_{ab(c)}=N\omega_{1(-)}|\mu_{ab(c)}|^2/(2\hbar c\epsilon_0)$, $R_j(\omega)=\omega+R_j'(j=1,2,3)$, and $S(\omega)=[\kappa_{ab}(R_1R_3-|\Omega_2|^2)-\kappa_{ac}(R_2R_3-|\Omega_+|^2)]^2+4\kappa_{ab}\kappa_{ac}|\Omega_+|^2|\Omega_2|^2$. The physical interpretation of Eq. (6a) is rather clear. $\mathrm{Im}(K_\pm^{(0)})$ describes absorption coefficient of the probe and mixing fields, $K_\pm^{(1)}$ determines the propagation velocity, and $K_\pm^{(2)}$ represents the group-velocity dispersion. We define absorption coefficient $\alpha_\pm=2\,\mathrm{Im}(K_\pm^{(0)})$.

A complete description of probe and mixing fields by performing inverse Fourier transform often requires much complicated calculation. However, considerable physical insight is gained by considering the approximate analytic solution, which takes a simple form if we focus on the adiabatic regime. Within an adiabatic framework, the power-series expansion of $K_\pm(\omega)$ and $U_\pm(\omega)$ on ω converge rapidly. We substitute the power-series expansion of $K_\pm(\omega)$ and $U_\pm(\omega)$ on ω into Eqs. (5a) and (5b). In order that Eqs. (5a) and (5b) are self-consistent for the wave propagating to the right, we can take approximate inverse Fourier transform by neglecting $O(\omega^2)$ in $K_\pm(\omega)\simeq K_\pm^{(0)}+K_\pm^{(1)}\omega$ and $O(\omega^1)$ in $U_\pm(\omega)\simeq U_\pm^{(0)}$. This gives

$$\Omega_1(x,t)=\tilde{\Omega}_1^+(\eta_+)-\tilde{\Omega}_1^-(\eta_-), \tag{7a}$$

$$\Omega_-(x,t)=\tilde{\Omega}_-^+(\eta_+)-\tilde{\Omega}_-^-(\eta_-),$$

$$=U_+^{(0)}\tilde{\Omega}_1^+(\eta_+)-U_-^{(0)}\tilde{\Omega}_1^-(\eta_-) \tag{7b}$$

where $\eta_\pm=t-xK_\pm^{(1)}$, group velocity is determined by the relationship $1/V_g^\pm=\mathrm{Re}(K_\pm^{(1)})$, and $\tilde{\Omega}_-^\pm(\eta_\pm)=\Omega_-^\pm(\eta_\pm)\times\exp[ixK_\pm(0)]$. With the help of Eqs. (7a) and (7b), we find $\Omega_-^\pm(t)$ satisfy the following relation:

$$\Omega_-^\pm(t)=\frac{U_\mp^{(0)}[\Omega_-(0,t)-U_\pm^{(0)}\Omega_1(0,t)]}{U_+^{(0)}-U_-^{(0)}}. \tag{8}$$

We can obtain the relationship $\tilde{\Omega}_-^\pm(\eta_\pm)=U_\pm^{(0)}\tilde{\Omega}_1^\pm(\eta_\pm)$ from Eq. (7b). If the given input fields $\Omega_1(0,t)$ and $\Omega_-(0,t)$ satisfy the condition $\Omega_-(0,t)/\Omega_1(0,t)=U_+^{(0)}$ or $\Omega_-(0,t)/\Omega_1(0,t)=U_-^{(0)}$, we obtain $\Omega_-^+(t)=0$ or $\Omega_-^-(t)=0$. The result demonstrates that there exists no K_+ or K_- mode excitation in the waveguide. In this paper, we consider that no input mixing field at $x=0$, i.e. $\Omega_1(0,t)=0$. This leads $\Omega_-(0,t)/\Omega_1(0,t)\neq U_\pm^{(0)}$. Equation (8) reduces to the simple expression $\Omega_-^\pm(t)=U_\mp^{(0)}\Omega_-(0,t)/(U_+^{(0)}-U_-^{(0)})$. So both K_- and K_+ modes will be excited in the semiconductor quantum well medium. The two modes will quickly walk off each other due to K_+ and K_- modes having different group velocities and absorption coefficients for the typical parameters. In Figs. 2 and 3, we plot α_+ as a function of Rabi frequency Ω_+/γ_1 (Ω_2/γ_1) with different values of decay rate γ_3. From Figs. 2 and 3, we find that, in the appropriate parameter regimes, α_+ is reduced due to electron spin coherence and $K_-(\omega)$ mode decays quickly. Thus, we can neglect the $K_-(\omega)$ mode after a very short propagation distance. The mixing field under these conditions takes the form $\Omega_1(x,t)=\tilde{\Omega}_1^+(\eta_+)-\tilde{\Omega}_1^-(\eta_-)\simeq\tilde{\Omega}_1^+(\eta_+)=\Omega_1^+\exp[ixK_+(0)]$ and the probe field takes the form $\Omega_-(x,t)\simeq\tilde{\Omega}_-^+(\eta_+)=\Omega_-^+(\eta_+)\exp[ixK_\pm(0)]$, so we obtain

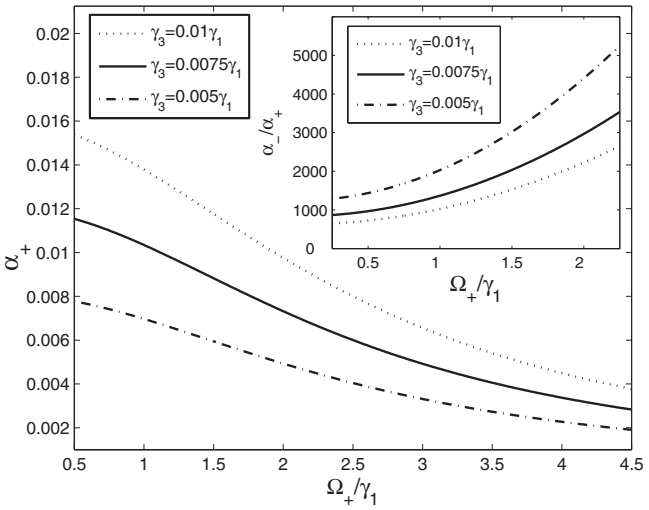

FIG. 2. α_+ as a function of Rabi frequency Ω_+/γ_1 with different values of decay rate γ_3. We have selected $\hbar\gamma_1=65$ μeV, $\gamma_2=\gamma_1$, $\Delta_1=\Delta_3=\Delta_-=0$, $\Omega_2/\gamma_1=2.5$, and $\kappa_{ab}=\kappa_{ac}=10\gamma_1$. Inset shows α_-/α_+ as a function of Rabi frequency Ω_+/γ_1 with different values of decay rate γ_3.

$$\Omega_-=U_+^{(0)}\Omega_1, \tag{9}$$

where Ω_-^+ and Ω_1^+ are slowly varying functions.

The linear susceptibility are obtained

$$\chi_-=\frac{N|\mu_{ac}|^2}{\hbar\epsilon_0}\frac{\Omega_2\Omega_+^*\Omega_1/\Omega_-+R_2'R_3'-|\Omega_+|^2}{R_1'R_2'R_3'-R_1'|\Omega_+|^2-R_2'|\Omega_2|^2} \tag{10}$$

and

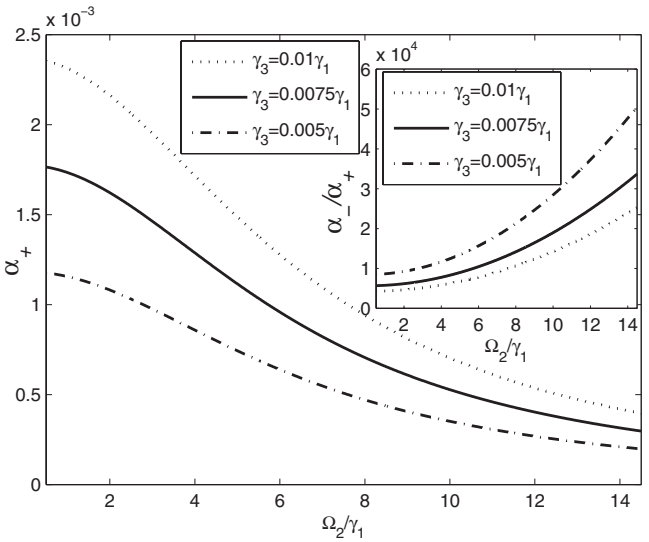

FIG. 3. α_+ as a function of Rabi frequency Ω_2/γ_1 with different values of decay rate γ_3. We have selected $\hbar\gamma_1=65$ μeV, $\gamma_2=\gamma_1$, $\Delta_1=\Delta_3=\Delta_-=0$, $\Omega_+/\gamma_1=6.5$, and $\kappa_{ab}=\kappa_{ac}=10\gamma_1$. Inset shows α_-/α_+ as a function of Rabi frequency Ω_2/γ_1 with different values of decay rate γ_3.

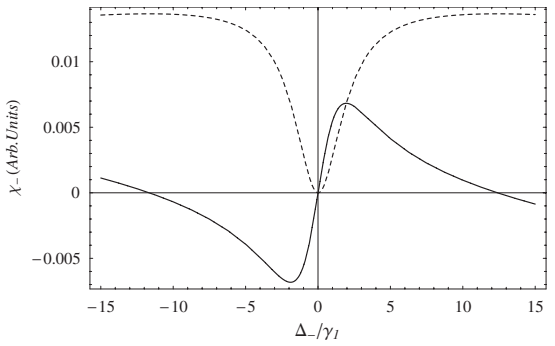

FIG. 4. Real and imaginary parts of the probe field susceptibility χ_- as a function of detuning Δ_-/γ_1. The imaginary part (dashed line) of susceptibility χ_- describes absorption. The real part (full line) of susceptibility χ_- describes the refraction.

$$\chi_1 = \frac{N|\mu_{ab}|^2}{\hbar\epsilon_0}\frac{R_1'R_3' - |\Omega_2|^2 + \Omega_+\Omega_2^*\Omega_-/\Omega_1}{R_1'R_2'R_3' - R_1'|\Omega_+|^2 - R_2'|\Omega_2|^2}, \tag{11}$$

where χ_- and χ_1 are the probe and mixing fields susceptibility, respectively. For giving the more intuitionistic characteristic of susceptibility, we present Figs. 4 and 5. In Fig. 4, we take $\hbar\gamma_1 = 65\ \mu$eV, $\gamma_2 = \gamma_1$, $\gamma_3/\gamma_1 = 10^{-4}$, $\Omega_+/\gamma_1 = 8.5$, $\Omega_2/\gamma_1 = 8.5$, $\Delta_1 = \Delta_2 = 0.01\gamma_1$, and $N|\mu_{ac}|^2/\hbar\epsilon_0 = 1$. It is shown that a sharp "hole" in the absorption line at $\Delta_- = 0$. In Fig. 5, we select $\Omega_+ = \Omega_2 = \gamma_1$ and the other parameters are the same as Fig. 4. From Fig. 5, one can control the absorption of the probe field by changing detuning Δ_- and obtain a wide transparency window. Figures 4 and 5 also show the steep positive dispersion near zero detuning which indicate the group velocity can be effectually reduced. The lowest-order nonlinear susceptibility of the mixing field is

$$\chi_1^N = \frac{N|\mu_{ab}|^2}{\hbar\epsilon_0}\frac{I_{11}(|I_{11}|^2 + |I_{22}|^2 + |I_{33}|^2)}{I_{44}|I_{44}|^2}, \tag{12}$$

where $I_{11} = R_1'R_3' - |\Omega_2|^2 + \Omega_+\Omega_2^*U_+^{(0)}$, $I_{22} = \Omega_2\Omega_+^* + (R_2'R_3' - |\Omega_+|^2)U_+^{(0)}$, $I_{33} = R_1'\Omega_+^* + R_2'\Omega_2^*U_+^{(0)}$, and $I_{44} = R_1'R_2'R_3' - R_1'|\Omega_+|^2 - R_2'|\Omega_2|^2$. In general, the high-order nonlinear polarization is very small. Therefore, the lowest-order nonlinear polarization is sufficient to describe the nonlinear effects.

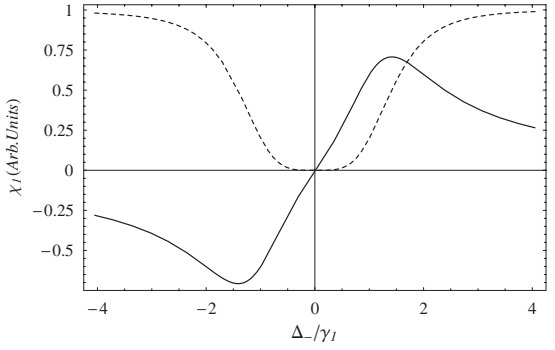

FIG. 5. Real and imaginary parts of the mixing field susceptibility χ_1 as a function of detuning Δ_-/γ_1. The imaginary part (dashed line) of susceptibility χ_1 describes absorption. The real part (full line) of susceptibility χ_1 describes the refraction.

Next, the lowest-order nonlinear susceptibility is included in propagation equation and the propagation properties of the mixing field are discussed.

III. SOLITON SOLUTIONS AND NONLINEAR DYNAMICS

The next task is to analyze the effect of Kerr nonlinear on the mixing field evolution. Under the slowly varying envelope approximation, the nonlinear propagation equation of the mixing field in the quantum well waveguide can be written as [30]

$$\frac{\partial}{\partial x}\Omega_1 + \frac{1}{V_g^+}\frac{\partial}{\partial t}\Omega_1 + i\frac{K_+^{(2)}}{2}\frac{\partial^2}{\partial t^2}\Omega_1 + \frac{\alpha_+}{2}\Omega_1 = ik_1\frac{\chi_1^N}{2}|\Omega_1|^2\Omega_1, \tag{13}$$

where $k_1 = \omega_1/c$ and c is the velocity of light in vacuum. By defining $\xi = x$ and $\eta = t - x/V_g^+$ and using variable substitution $W = \frac{\omega_1}{2c}\frac{N|\mu_{ab}|^2}{\hbar\epsilon_0}\frac{(|I_{11}|^2+|I_{22}|^2+|I_{33}|^2)I_{11}}{I_{44}|I_{44}|^2}$, we can arrive a simple expression for Eq. (13)

$$i\frac{\partial}{\partial\xi}\Omega_1(\xi,\eta) - \frac{K_+^{(2)}}{2}\frac{\partial^2}{\partial\eta^2}\Omega_1(\xi,\eta) + \frac{\alpha_+}{2}\Omega_1(\xi,\eta) = W|\Omega_1(\xi,\eta)|^2\Omega_1(\xi,\eta). \tag{14}$$

This is the one-dimensional complex Ginzburg-Landau equation. It describes vast variety nonlinear phenomena, such as slightly unstable nonlinear waves and second-order phase transitions. In this equation, if all of the coefficients are real, Eq. (14) can be simplified to the real Ginzburg-Landau equation. Fortunately, the absorption coefficient α_+ is very small so it can be neglected in Eq. (14) (see Figs. 2 and 3). The numerical calculation demonstrates that $K_+^{(2)}$ and W have imaginary parts, but the imaginary parts are much smaller than the corresponding real parts, i.e., $K_+^{(2)} = K_{+r}^{(2)} + iK_{+i}^{(2)} \simeq K_{+r}^{(2)}$ and $W = W_r + iW_i \simeq W_r$, then Eq. (14) can be simplified to the standard nonlinear Schrödinger equation

$$i\frac{\partial}{\partial\xi}\Omega_1(\xi,\eta) - \frac{K_{+r}^{(2)}}{2}\frac{\partial^2}{\partial\eta^2}\Omega_1(\xi,\eta) = W_r|\Omega_1(\xi,\eta)|^2\Omega_1(\xi,\eta). \tag{15}$$

According to Refs. [59,60], the standard nonlinear Schrödinger equation admits bright soliton when $K_{+r}^{(2)}W_r > 0$ and dark soliton [localized nonlinear waves (or holes) existing on a stable continuous wave (or extended finite-width) background] when $K_{+r}^{(2)}W_r < 0$. N-order solitons ($N = 2,3,\ldots$) are also described by the general solution of Eq. (15). The single soliton is called fundamental soliton and the N soliton ($N = 2,3,\ldots$) is named as the higher-order soliton. And whether the solution to Eq. (15) is the bright soliton or the dark soliton depends on the sign of the product $K_{+r}^{(2)}W_r$. The solution of Eq. (15) is referred to as soliton solution because its shape does not change during its propagation. When $K_{+r}^{(2)}W_r > 0$, Eq. (15) has the bright soliton solution [59,60]

$$\Omega_1(\xi,\eta) = \Omega_{10}\,\mathrm{sech}(\eta/\tau)\exp(-i\xi W_r|\Omega_{10}|^2/2), \tag{16}$$

where the amplitude Ω_{10} and width τ are arbitrary constants, which are subjected only to the constraint $|\Omega_{10}\tau|^2 = K_{+r}^{(2)}/W_r$,

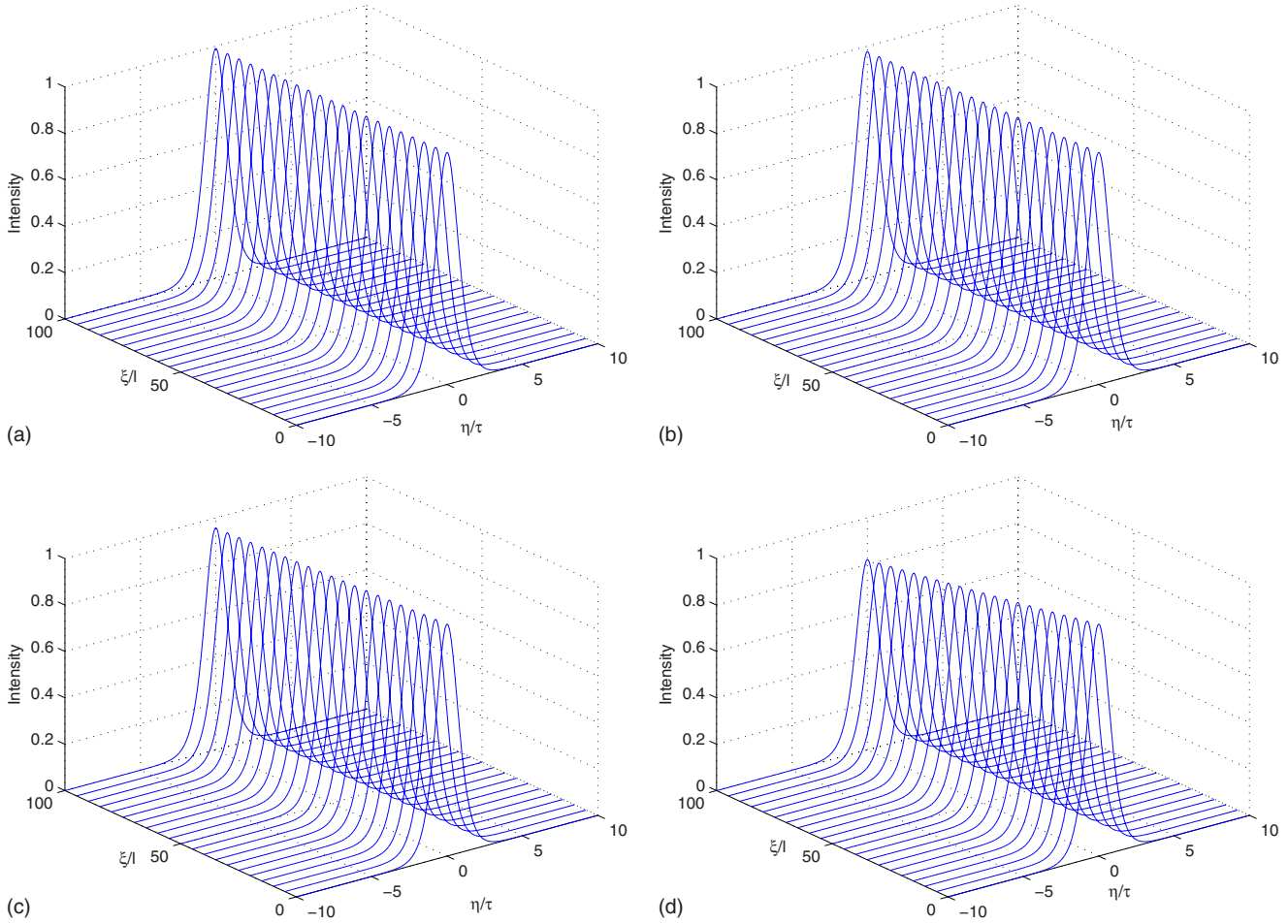

FIG. 6. (Color online) Space-time evolution of the soliton intensity with (a) $\gamma_3/\gamma_1=0.1\times10^{-4}$, (b) $\gamma_3/\gamma_1=0.5\times10^{-4}$, (c) $\gamma_3/\gamma_1=1\times10^{-4}$, and (d) $\gamma_3/\gamma_1=10\times10^{-4}$. Other parameters of (a), (c), and (d) are the same as (b), which are given in the main text.

and sech(η/τ) is the hyperbolic secant function. The function in this solution provides for the localization of the soliton. This means that if an initial pulse with pulse shape given by Eq. (16) is launched inside an ideal lossless waveguide, the pulse will propagate in the same manner as the single soliton pulse case, i.e., undistorted and without change in shape for long distances. The probe and mixing fields are related to bright fundamental soliton by Eq. (9), $\Omega_-(\xi,\eta)=U_+^{(0)}\Omega_1(\xi,\eta)$. The probe and mixing fields have considerably different carrier frequencies and have the same amplitude envelope, which clearly illustrate that the pulse shape can be bright soliton types. This displays the concept of matched soliton pairs.

In the next study, the numerical simulation on dynamic evolution of nonlinear propagation equation was investigated. Here, we focused on the one-dimensional nonlinearevolution Eq. (14). Using the initial pulse form Eq. (16), numerical simulation was carried out to solve Eq. (14). The split-step Fourier transform algorithm with constant time steps was used. First, we study the fundamental bright soliton evolution in the waveguide then we discuss the effect of electron spin coherence on soliton propagation. Second, we analyze the collision of two solitons under different initial conditions. With the help of the split-step Fourier transform algorithm, direct numerical simulations of Eq. (14) with the initial wave form (16) are performed in Fig. 6. In Fig. 6(b), we plot the relative soliton intensity of mixing field versus dimensionless η/τ and ξ/l and we select $\hbar\gamma_1=65$ μeV, $\gamma_2=\gamma_1$, $\gamma_3/\gamma_1=0.5\times10^{-4}$, $\Omega_2=2\Omega_2=2\gamma_1$, $\Delta_-=0.018\gamma_1$, $\Delta_1=-\Delta_2=180\gamma_1$, $\Delta_2=0.0095\gamma_1$, and $\kappa_{ab}=\kappa_{ac}=100\gamma_1$, then we obtain $\alpha_+\simeq4.16\times10^{-4}$ cm^{-1}, $W\simeq(4.57-0.003i)\times10^{-22}$ s^2 cm^{-1}, $K_+^{(2)}\simeq(2.32-0.01i)\times10^{-18}$ s^2 cm^{-1}, and $V_g^+/c\simeq0.02$. With above parameters, one obtains $K_{+r}^{(2)}W_r>0$, so the bright soliton can form in the quantum well waveguide. As shown in Fig. 6(b), the fundamental bright soliton can preserve its shape during its propagation. It is shown that fundamental bright soliton can propagate in the waveguide without absorption in Figs. 6(a) and 6(b). However, when electron spin-coherence decay increases, the bright soliton intensity reduces in a short propagation distance, which is shown in Figs. 6(c) and 6(d). These results can be explained as follows: states $|a\rangle$, $|b\rangle$, and $|d\rangle$ create a V-type system and the strong control field Ω_+ creates two dressed states $|\pm\rangle\propto|b\rangle\pm|d\rangle$. The weak mixing field Ω_1 exhibits two path transitions to the two dressed states. So the absorption of weak mixing field will be reduced due to quantum coherence with low electron spin-coherence decay. However, the quantum coherence can be destroyed due to the increasing electron spin-coherence decay. Then, we have also investigated the collision of two-soliton evolution with dif-

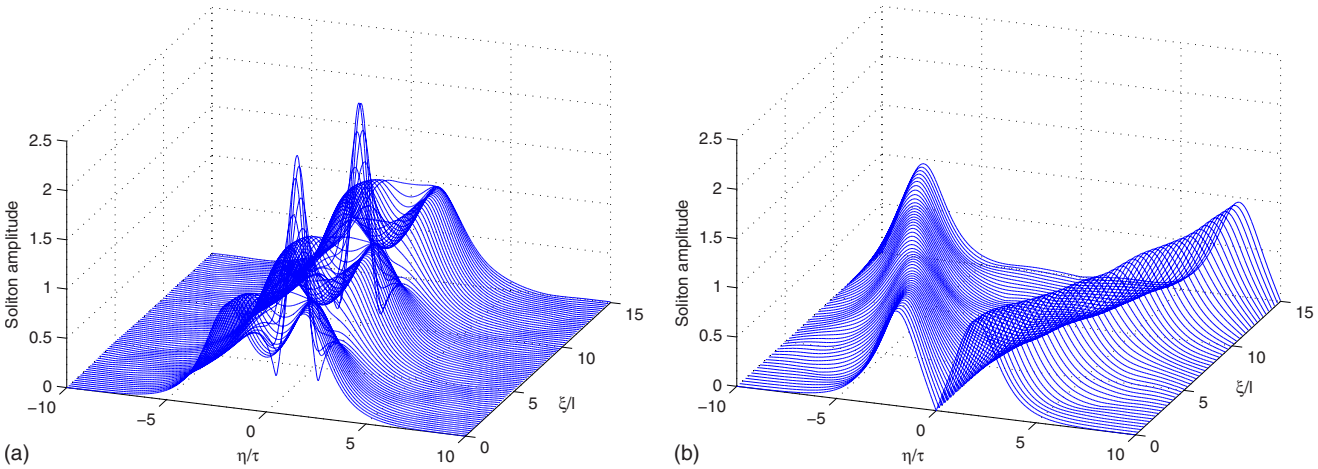

FIG. 7. (Color online) Evolution of two solitons collision showing the effects of solitons interaction for the same amplitude and different relative phases: (a) two solitons in phase and (b) two solitons out of phase.

ferent initial conditions by using numerical simulations as shown in Fig. 7. We have selected all the parameters that are the same as in Fig. 6(b). Figure 7(a) shows the evolution of a soliton pair with an initial separation for the same soliton amplitude and phase. In this case, the two solitons exhibit attraction interaction and periodically collide along the waveguide length. We clearly see that the solitons firstly collide and then recover their initial waveforms after the interaction in one period. When the solitons are out of phase and also have the same amplitudes, the interaction between two solitons is repellency, which is shown in Fig. 7(b). From Fig. 7(b), we see that two solitons walk into each other in an initial stage then separate from each other while recovering their initial waveforms. And their spacing increases with distance monotonically due to the repellency interaction.

IV. CONCLUSIONS

We have theoretically investigated the propagation properties of probe and mixing fields in a quantum well waveguide. Our scheme used lh transitions in the quantum well waveguide to induce electron spin coherence in the presence of two strong fields and a weak field. The results revealed that probe (or mixing) field consists of two modes with different group velocity and absorption. The long lifetime electron spin coherence could restrain absorption of weak field and enhance the nonlinear susceptibilities. Under the slowly varying envelope approximation, we discussed the propagation equation of weak field which includes the higher-order nonlinear term. Under appropriate conditions, the optical soliton pairs formed in the quantum well waveguide and freely propagated with slow group velocity. With the help of the split-step Fourier transform algorithm, the numerical procedure was used to study the simulation on dynamic evolution of soliton. Numerical simulation results clearly demonstrated that the soliton can propagate in the quantum well waveguide and the electron spin coherence can effect the propagation of soliton.

ACKNOWLEDGMENTS

The authors express their gratitude to the referee of the paper for his/her fruitful advice and comment, which significantly improved the paper. The research is supported in part by the National Natural Science Foundation of China (Grants No. 10904033 and No. 90503010), by program for talent introduction of Hubei Normal University under Grant No. 2008F10, by Educational Commission of Hubei Province of China under Grant No. D20092204, and by Natural Science Foundation of Hubei Province of China under Grant No. 2009CDA145. The authors would like to thank Prof. Wu Ying for helpful discussion and his encouragement.

[1] J. M. Kikkawa and D. D. Awschalom, Phys. Rev. Lett. **80**, 4313 (1998).
[2] J. M. Kikkawa, I. P. Smorchkova, N. Samarth, and D. D. Awschalom, Science **277**, 1284 (1997).
[3] D. D. Awschalom, N. Samarth, and D. Loss, *Semiconductor Spintronics and Quantum Computation* (Springer-Verlag, Berlin, 2002).
[4] B. E. Kane, Nature (London) **393**, 133 (1998).
[5] S. A. Wolf, D. D. Awschalom, R. A. Buhrman, J. M. Daughton, S. von Molnár, M. L. Roukes, A. Y. Chtchelkanova, and D. M. Treger, Science **294**, 1488 (2001).
[6] Kai-Mei C. Fu, C. Santori, C. Stanley, M. C. Holland, and Y. Yamamoto, Phys. Rev. Lett. **95**, 187405 (2005).
[7] G. Salis, Y. Kato, K. Ensslin, D. C. Driscoll, A. C. Gossard, and D. D. Awschalom, Nature (London) **414**, 619 (2001).
[8] M. Atature, J. Dreiser, A. Badolato, and A. Imamöglu, Nat. Phys. **3**, 101 (2007).
[9] A. S. Bracker, E. A. Stinaff, D. Gammon, M. E. Ware, J. G. Tischler, A. Shabaev, A. L. Efros, D. Park, D. Gershoni, V. L. Korenev, and I. A. Merkulov, Phys. Rev. Lett. **94**, 047402

(2005).
[10] A. Högele *et al.*, Appl. Phys. Lett. **86**, 221905 (2005).
[11] Y. Wu, E. D. Kim, X. Xu, J. Cheng, D. G. Steel, A. S. Bracker, D. Gammon, S. E. Economou, and L. J. Sham, Phys. Rev. Lett. **99**, 097402 (2007).
[12] M. H. Mikkelsen, J. Berezovsky, N. G. Stoltz, L. A. Coldren, and D. D. Awschalom, Nat. Phys. **3**, 770 (2007).
[13] Z. Chen, S. G. Carter, R. Bratschitsch, P. Dawson, and S. T. Cundiff, Nat. Phys. **3**, 265 (2007).
[14] S. E. Harris, Phys. Today **50**(7), 36 (1997).
[15] M. D. Lukin, Rev. Mod. Phys. **75**, 457 (2003); G. S. Agarwal and W. Harshawardhan, Phys. Rev. Lett. **77**, 1039 (1996); M. Fleischhauer, A. Imamoglu, and J. P. Marangos, Rev. Mod. Phys. **77**, 633 (2005).
[16] A. Imamoğlu, Opt. Commun. **179**, 179 (2000).
[17] J. H. Xu, G. C. La Rocca, F. Bassani, D. Wang, and J. Y. Gao, Opt. Commun. **216**, 157 (2003).
[18] G. X. Li, F. L. Li, and S. Y. Zhu, Phys. Rev. A **64**, 013819 (2001).
[19] H. Jing, X. J. Liu, M. L. Ge, and M. S. Zhan, Phys. Rev. A **71**, 062336 (2005).
[20] X. M. Hu and J. S. Peng, J. Phys. B **33**, 921 (2000).
[21] S. E. Harris, Phys. Rev. Lett. **62**, 1033 (1989).
[22] O. A. Kocharovskaya and P. Mandel, Phys. Rev. A **42**, 523 (1990).
[23] A. Imamoğlu, J. E. Field, and S. E. Harris, Phys. Rev. Lett. **66**, 1154 (1991).
[24] M. Xiao, Y. Q. Li, S. Z. Jin, and J. Gea-Banacloche, Phys. Rev. Lett. **74**, 666 (1995).
[25] R. Binder and M. Lindberg, Phys. Rev. Lett. **81**, 1477 (1998).
[26] Y. Wu, J. Saldana, and Y. F. Zhu, Phys. Rev. A **67**, 013811 (2003).
[27] Y. Wu and X. Yang, Phys. Rev. A **62**, 013603 (2000).
[28] L. Deng, M. Kozuma, E. W. Hagley, and M. G. Payne, Phys. Rev. Lett. **88**, 143902 (2002).
[29] Y. Wu and L. Deng, Phys. Rev. Lett. **93**, 143904 (2004).
[30] G. P. Agrawal, *Nonlinear Fiber Optics* (Academic, New York, 2001), Chap. 5.
[31] H. A. Haus and W. S. Wong, Rev. Mod. Phys. **68**, 423 (1996).
[32] G. T. Adamashvili, C. Weber, A. Knorr, and N. T. Adamashvili, Phys. Rev. A **75**, 063808 (2007).
[33] W.-X. Yang, J.-M. Hou, and R.-K. Lee, Phys. Rev. A **77**, 033838 (2008).
[34] X. T. Xie, W. Li, J. Li, W. X. Yang, A. Yuan, and X. Yang, Phys. Rev. B **75**, 184423 (2007); J.-B. Liu, X.-Y. Lü, P. Huang, C.-L. Ding, and J. Li, Eur. Phys. J. B **63**, 479 (2008); J.-B. Liu, X.-T. Xie, and Y. Wu, Europhys. Lett. **89**, 17006 (2010).
[35] Y. Wu and X. Yang, Appl. Phys. Lett. **91**, 094104 (2007).
[36] B. Wu, J. Liu, and Q. Niu, Phys. Rev. Lett. **88**, 034101 (2002).
[37] L. Salasnich and B. A. Malomed, Phys. Rev. A **74**, 053610 (2006).
[38] H. E. Nistazakis, D. J. Frantzeskakis, P. G. Kevrekidis, B. A. Malomed, and R. Carretero-González, Phys. Rev. A **77**, 033612 (2008).
[39] H. Xiong, S. Liu, G. Huang, and Z. Xu, J. Phys. B **35**, 4863 (2002).
[40] A. V. Rybin, I. P. Vadeiko, and A. R. Bishop, Phys. Rev. E **72**, 026613 (2005); G. Huang, L. Deng, and C. Hang, *ibid.* **72**, 036621 (2005).
[41] X.-J. Liu, H. Jing, and M.-L. Ge, Phys. Rev. A **70**, 055802 (2004).
[42] L. Deng, M. G. Payne, G. Huang, and E. W. Hagley, Phys. Rev. E **72**, 055601(R) (2005).
[43] Y. Wu, Phys. Rev. A **71**, 053820 (2005).
[44] D. N. Christodoulides and R. I. Joseph, Opt. Lett. **13**, 53 (1988).
[45] Y. Barad and Y. Silberberg, Phys. Rev. Lett. **78**, 3290 (1997).
[46] D. Rand, I. Glesk, C.-S. Brès, D. A. Nolan, X. Chen, J. Koh, J. W. Fleischer, K. Steiglitz, and P. R. Prucnal, Phys. Rev. Lett. **98**, 053902 (2007).
[47] M. Segev, G. C. Valley, B. Crosignani, P. Di Porto, and A. Yariv, Phys. Rev. Lett. **73**, 3211 (1994).
[48] J. U. Kang, G. I. Stegeman, J. S. Aitchison, and N. Akhmediev, Phys. Rev. Lett. **76**, 3699 (1996).
[49] M. Delqué, T. Sylvestre, H. Maillotte, C. Cambournac, P. Kockaert, and M. Haelterman, Opt. Lett. **30**, 3383 (2005).
[50] L.-G. Si, W.-X. Yang, J.-B. Liu, J. Li, and X. Yang, Opt. Express **17**, 7771 (2009).
[51] T. Li, H. Wang, N. Kwong, and R. Binder, Opt. Express **11**, 3298 (2003).
[52] S.-W. Chang, H. L. Chuang, C. J. Chang-Hasnain, and H. Wang, J. Opt. Soc. Am. B **24**, 849 (2007).
[53] P. Palinginis, F. Sedgwick, S. Crankshaw, M. Moewe, and C. J. Chang-Hasnain, Opt. Express **13**, 9909 (2005).
[54] X. Yang, Z. Li, and Y. Wu, Phys. Lett. A **340**, 320 (2005).
[55] Y. Ohno, R. Terauchi, T. Adachi, F. Matsukura, and H. Ohno, Phys. Rev. Lett. **83**, 4196 (1999).
[56] Y. Wu, M. G. Payne, E. W. Hagley, and L. Deng, Opt. Lett. **29**, 2294 (2004).
[57] F. G. Sedgwick, Ph.D. thesis, University of California, 2008.
[58] M. O. Scully and M. S. Zubairy, *Quantum Optics* (Cambridge University Press, Cambridge, England, 1997), Chap. 5.
[59] Y. S. Kivshar and B. Luther-Davies, Phys. Rep. **298**, 81 (1998).
[60] J. Satsuma and N. Yajima, Prog. Theor. Phys. **55**, 284 (1974).